Langmuir and Grafted Monolayers of Photochromic Amphiphilic Monodendrons of Low Generations

Kirsten L. Genson,[†] **Jason Holzmuller,**[†] **Ovette F. Villacencio,**[‡] **Dominic V. McGrath,**[‡] **David Vaknin,**[§] **and Vladimir V. Tsukruk***[,†]

Department of Materials Science and Engineering and Ames Laboratory and Department of Physics and Astronomy, Iowa State University, Ames, Iowa 50011, and Department of Chemistry, University of Arizona, P.O. Box 210041, Tucson, Arizona 85721

Four generations of monodendrons with multiple dodecyl alkyl tails (**AA-N**, N representing number of alkyl tails from 1 to 8), an azobenzene spacer group, and a carboxylic acid polar head have been studied at the air–water and air–solid interface using AFM, GIXD, X-ray reflectivity, and UV–vis spectrometry. The one and two tail molecules formed orthorhombic lateral packing with long-range intramonolayer ordering. Good agreement between molecular models and thickness measurements indicated that the one and two tail molecules orient along the surface normal. The increase in the cross-sectional mismatch caused by the presence of the multiple chains for the higher generations disrupted the long-range ordering and forced the alkyl tails to adopt quasi-hexagonal structure. The higher generations (**AA-4** and **AA-8**) formed a kinked structure with the alkyl tails oriented perpendicular to the surface with the azobenzene group tilted at a large degree toward the surface. The photoisomerization behavior in dilute solutions, at the air–water interface, and for grafted layers demonstrated that lower generation monodendrons maintained the photochromic behavior after chemical grafting to the silicon substrates, although the confinement of the molecules in monolayers significantly increased the reorganization time.

Introduction

One of the challenges in the field of nanotechnology is controlling the selective response of thin films, especially organized surface monolayers.[1] Recent investigations in this area have concentrated on tailoring the response of a thin film to environmental stimuli at the nanometer scale.[2] In this regard, molecules with azobenzene fragments have been considered as potential components of films with selective light-triggered responses. Indeed, a multitude of studies focused on various molecules with azobenzene fragments such as holographic media[3] for optical storage,[4] as reversible optical waveguides,[5] for photoalignment of liquid crystal systems,[6] and for drug delivery.[7] The azobenzene group is attractive due to the two stable isomers it assumes upon selective wavelength stimuli. The main complication of the inclusion of photoresponsive molecules in selective response monolayers is the preservation of the full and fast isomerization response.[8] Deposition of thin surface films onto solid supports often restricts the mobility of the photochromic fragments within the molecular architecture and thin films, thereby reducing the overall response and the reversibility. The tilted orientation of azobenzene containing molecules in self-assembled monolayers reduced the surface coverage (50–60%) and lowered the monolayer thickness, thereby resulting in a slight increase in thickness during photoisomerization.[9]

Similarly, the tailoring of material's properties, especially the packing structure, by tailoring the molecular architecture has been discussed in detail.[10] Since the discovery of dendrimers, a multitude of applications has been considered, but the overall theme of the studies has been the understanding of the exponential increase in end groups on the overall material's behavior and properties.[11] Many studies focused on higher generation monodendrons and dendrimers with little attention paid to the lower generations.[12,13] The inclusion of hydrophobic and hydrophilic fragments creating an amphiphilic balance facilitates the study of the molecules in ordered monolayers at the air–water interface.[14] Combining experimental techniques at both the air–water and the air–solid interface provides in-depth understanding of the molecular ordering and rearrangement of fragments at both interfaces. To facilitate the grafting of the photochromic monodendrons onto solid substrates while preserving the photoisomerization of the molecules, we have investigated several chemically disparate polar heads. Previously, we showed that the attachment of a bulky crown ether polar head to photochromic monodendrons created a kinked structure at the air–water and air–solid interface and preserved photochromic properties under a balance of cross-sectional areas of the bulky polar groups and dendritic alkyl shells.[15]

In this paper, we report on the interfacial behavior of four generations of photochromic monodendrons, their molecular ordering, and its contribution to reversible photoisomerization at interfaces. Replacement of the bulky polar group in previously studied monodendrons[15] with a smaller functional group (i.e., a traditional polar group) is expected to promote chemical grafting to solid surfaces while preserving the cross-sectional area necessary for complete and reversible photoisomerization within the surface monolayers. The attachment of a traditional

* Corresponding author: vladimir@iastate.edu.
† Department of Materials Science and Engineering, Iowa State University.
‡ University of Arizona.
§ Ames Laboratory and Department of Physics and Astronomy, Iowa State University.

carboxylic polar head to photochromic monodendrons generated a cross-sectional mismatch favorable for the azobenzene spacer group. In addition to the first direct observation of the trans−cis photoisomerization in Langmuir monolayers, photoisomerization studies demonstrated that lower generation monodendrons maintained the photochromic behavior after chemical grafting to the silicon substrates although with increased reorganization time.

Experimental Procedures

Liquid surface measurements were performed on monomolecular films spread on a temperature controlled, Teflon trough. The trough was placed in a helium-filled chamber for the duration of the experiments to reduce the background scattering and oxidation of the monolayer. A combination of grazing incident X-ray diffraction (GIXD) (in-plane and rod-scans) and X-ray reflectivity experiments were conducted on a liquid-surface X-ray spectrometer at the 6ID beam line at the Advanced Photon Source synchrotron at Argonne National Laboratory according to the usual procedure.[16−18] X-ray reflectivity measurements of spread monolayers directly under UV illumination were carried out on a home-built liquid−surface reflectometer. The incident beam (Cu Kα; $\lambda = 1.5404$ Å) is selected from the white beam of a Cu-rotating-anode generator (UltraX1-18; Rigaku) by Bragg reflection from the (111) planes of a Ge single-crystal monochromator. Experimental details are available in the Supporting Information. The data are presented in reciprocal space ($\mathbf{Q}$) with $\mathbf{Q}_{xy}$ representing the vector in the H and K direction and $\mathbf{Q}_z$ representing the vector in the L direction. During the X-ray reflectivity experiments, the H and K vector remains zero, and the incident and reflected angles are increased equivalent degrees to scan along the L direction. During the GIXD experiments, the incident angle is fixed below the critical angle to ensure total reflectance as the H and K components ($\mathbf{Q}_{xy}$) are studied to determine the diffraction pattern of the sample. The L component ($\mathbf{Q}_z$) of the diffracted vector is fixed at different azimutal angles to discern the tilted behavior of the diffracting molecular fragments. Inversely, the H and K components are fixed and the L component is increased at reflex points to further characterize the tilt behavior and ordering of the diffracting molecules. Experimental setup and details regarding the X-ray reflectivity and GIXD are described in previous publications.[15] A downstream Si double-crystal monochromator was used to select the X-ray beam at the desired energy ($\lambda = 0.0772$ nm).

Monomolecular films of the amphiphilic compounds were prepared by the Langmuir technique on an RK-1 trough (Riegel and Kirstein, GmbH) located in a laminar flow hood. The compounds were dissolved in chloroform (Fisher, reagent grade) to concentrations of 0.5−1.0 mmol/L. The solution was spread over the water subphase (NanoPure, >18 MΩ cm). Monolayers were deposited on a cleaned silicon wafer[19,20] (Semiconductor Processing Co.) of the {100} orientation, following the usual LB procedure.[21] Cast films of the **AA-2** and **AE-1** molecules were deposited on clean quartz slides from dilute chloroform solutions. The films were annealed at 120 °C for 60 min under vacuum, then rinsed 3 times in chloroform and dried under dry nitrogen. The samples were placed in a dark room and illuminated with 365 nm light for different periods of time.

The UV−vis spectra of 0.01 mmol/L solutions in chloroform were obtained with a Shimadzu-1601 spectrometer. A Blak-Ray ultraviolet lamp (UVP, Model B-100 AP, 100W) equipped with both a 365 nm band-pass filter and a 310 nm long-pass filter was used to illuminate the solutions at a distance of 0.4

m. Ellipsometric measurements of monolayer thickness were performed on a COMPEL Automatic Ellipsometer (InOmTech, Inc.). Imaging of the monolayers was carried out using atomic force microscopy (AFM) (Multimode and Dimension-3000, Digital Instruments), in tapping mode according to an experimental procedure described in detail earlier.[22] The geometrical parameters of all molecules were estimated from molecular models built with the Cerius[2] 3.8 package on a SGI workstation by using the Dreiding 2.21 force field library and with the Materials Studio 3.0 package using the PVCC force field library. Molecular models were treated with a molecular dynamics and minimization procedure to obtain molecular conformations with minimized energy for geometrical dimension calculations.

Results and Discussion

Photoisomerization in Solution. The **AA-N** (N represents the number of attached alkyl tails) molecules consist of a carboxylic acid headgroup, an azobenzene spacer group, and multiple dodecyl alkyl tails. The number of tails increases from one for (4-dodecyloxyphenylazo)benzoic acid (**AA-1**), to two, four, and eight for the second, third, and fourth generations of a dendritic series (Figure 1). Comparison the single-tail molecule with an epoxy terminated reference molecule (**AE-1**, Figure 1) has demonstrated that the bulkier polar head broadened the alkyl tail packing structure. The synthesis of the compounds is presented elsewhere.[23] The photochromic isomerization of all four generations was readily observed in dilute solutions. In ambient light conditions, the $\pi−\pi^*$ absorbance band was observed at 365 nm, denoting that the **AA-N** molecules are in the trans isomer, with an additional peak observed at 290 nm attributed to the phenyl rings in the dendritic shell (Figure 2a).[24] After 1 min illumination with a 365 nm lamp, the absorbance band at 365 nm was greatly diminished, and additional absorbance bands were discerned at 318 and 445 nm, indicative of the transition from the trans to the cis isomer for all four generations (Figure 2b).

Surface Behavior of Langmuir Monolayers. All four molecules displayed classic amphiphilic behavior at the air−water interface with a sharp increase in surface pressure as the molecular area was reduced (Figure 3). **AA-1** had a higher than expected alkyl-chain limiting cross-sectional area of 0.24 nm² per molecule, while the three highest generations were observed to roughly follow the expected value of 0.20 nm² per alkyl tail with 0.36, 0.98, and 1.50 nm² for **AA-2**, **AA-4**, and **AA-8**, respectively. The molecular areas calculated from the Langmuir isotherms were in good agreement with the cross-sectional areas calculated from molecular models and GIXD data, concluding that all generations formed complete monolayers at the air−water interface at moderate surface pressures. The deviation of the one tail molecule from the expected molecular area indicated that a single alkyl tail does not control the limiting cross-sectional area, which is increased due to the presence of the bulky photochromic group and the polar head. The surface area per molecule rose with the increasing number of akyl tail in dendritic shells virtually doubling for each generation (Figure 3). In the end, the polar head and photochromic spacer had little influence on the cross-sectional area for the molecule with multiple (>2) alkyl tails in the dendritic shell.

Molecular Ordering in Langmuir Monolayers. The arrangement of the molecular fragments within Langmuir monolayers was revealed by X-ray reflectivity studies (Figure 4). The two-tail molecules (**AA-2**) had a single, well-defined minimum and an additional minimum at higher $\mathbf{Q}_z$ for lower surface pressure (Figure 4a). The lower $\mathbf{Q}_z$ minima became less defined
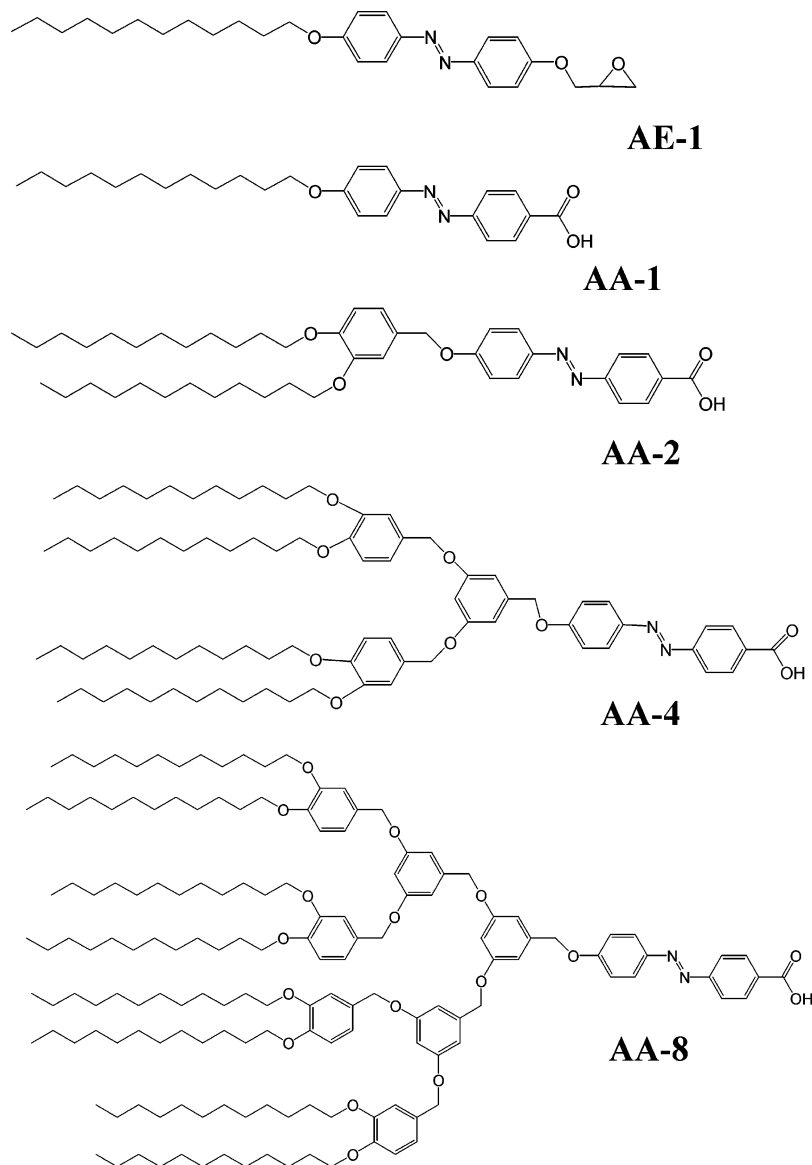
Figure 1. Chemical formulas of AA-N.

at higher surface pressures, indicating no clear transition between the focal group and the alkyl tails. Dissimilarly, **AA-4** had two defined minima at low and high surface pressures with less definition of the minima observed for the intermediate pressure (Figure 4b). The eight-tail molecule (**AA-8**) possessed a single defined minimum for the monolayer at moderate pressure with no distinct minima at low and high surface pressures (Figure 4c).

The data for **AA-2** and **AA-4** were modeled using a two-box model for electron density distribution along the surface normal at all surface pressures as well as the two lower surface pressures of **AA-8** (Table 1S and Figure 5; S refers to Supporting Information). The polar headgroup and the azobenzene fragment composed the first box with higher electron density, and the attached alkyl tails are located in the second box. The length of the focal group and proximity to the spacer group reduced the contrast between the fragments, thereby confining the fragments within one box. Previous studies of similar molecules in addition to lower generations demonstrated that the relative size of the polar group to the bulky spacer group was near the surface roughness calculated for the box models, thereby predicting a two box model more favorable than a three box model.[15,25] The highest surface pressure of **AA-8** was modeled

using a one box model, indicating that the contrast between the focal group and the eight attached alkyl tails diminished.

Comparison of the electron density distribution for all molecules as a function of surface pressure applied to the Langmuir monolayers suggests that the alkyl tails and azobenzene groups undergo the most dramatic rearrangements under different conditions. The one tail molecules had lower electronic densities calculated for the highest pressure indicative of an early monolayer collapse into a domain structure as was demonstrated before.[25] This molecule within the monolayer was composed of a vertically oriented azobenzene group and highly tilted alkyl tail (Figure 5d). This molecular ordering provided the appropriate balance between cross-sectional areas of the bulky azobenzene group and a single alkyl tail.

Comparison of this model to the electron density distribution for the **AA-2** molecule with two alkyl tails showed significant structural reorganization (Figure 5). Two alkyl tails became oriented vertically in a register with the azobenzene group due to a change in the cross-sectional mismatch of the azobenzene group and alkyl tails. As the monolayer compressed, the focal groups became more densely packed in addition to 15% lengthening in the vertical direction caused by lateral compression (Table 1S). The length of the alkyl tail box remained
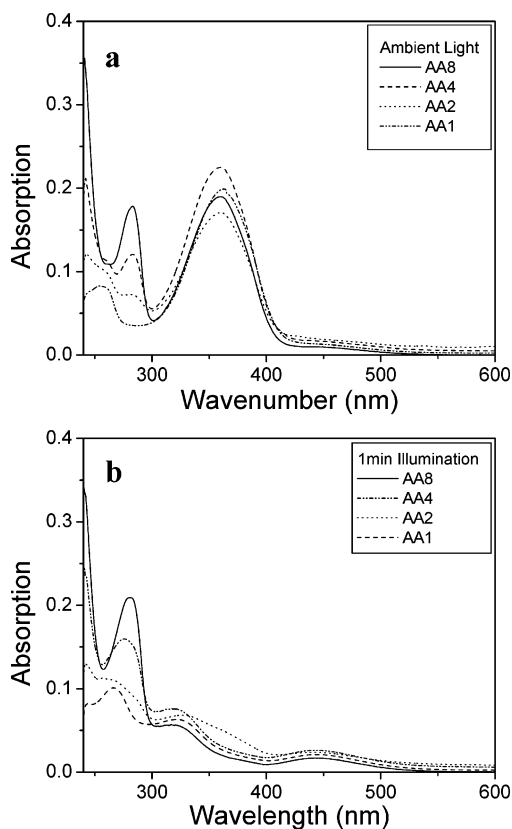
Figure 2. UV∼vis spectra for AA-N in dilute solution in a) ambient conditions and b) after 1 min illumination with 365 nm UV wavelength.
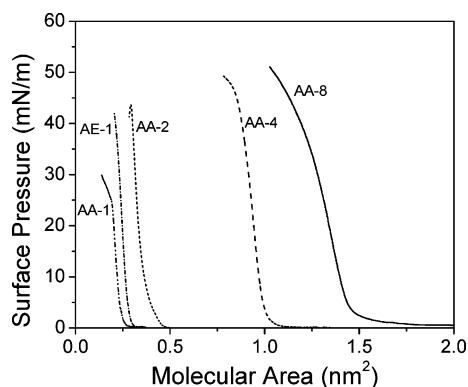

Figure 3. The $\pi-A$ isotherms for all molecules demonstrated a classic amphiphilic behavior with lower generations deviating from expected molecular area trend.

consistent with the vertically oriented fully extended chains, although the electronic density decreased for the highest surface pressure, suggesting that the monolayer collapsed into a domain structure at 20 mN/m. The electron density distribution calculated for the **AA-4** molecule was similar to the two tail molecule (Figure 5). At higher pressure, the second box for the four tail molecule reduced in length as the electronic density increased as expected for densely packed alkyl tails (Table 1S). At the lowest surface pressure, the monolayer of **AA-8** displayed a similar trend to the **AA-4** molecule. At the highest surface pressure, the denser monolayer slightly decreased in overall thickness, suggesting that the molecule adopted a tilted orientation to achieve a densely packed structure.

Further insight into the packing behavior of the alkyl tails was discerned from GIXD (in-plane and rod) experiments (Figures 6 and 7). As shown previously, **AA-1** formed a herringbone structure at the air−water interface with a relatively
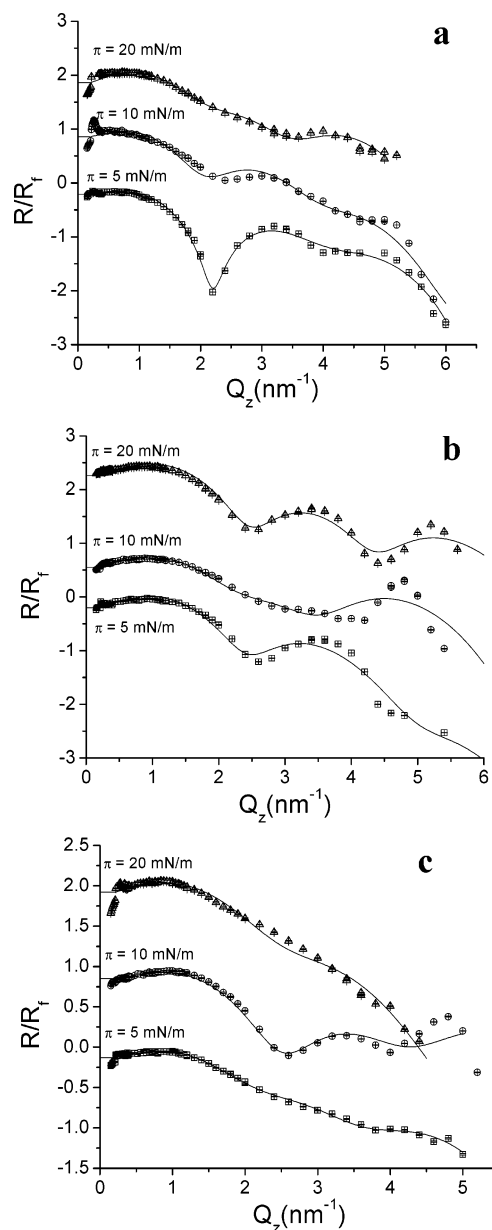

Figure 4. The X-ray reflectivity data of a) AA-2, b) AA-4 and c) AA-8 at all studied surface pressures.

large area per tail determined by GIXD.[25] Four sharp, intense peaks were observed at all surface pressures and were indexed as the (1,1), (2,0), (2,1), and (3,1) peaks. The alkyl tails were determined to be packed in an orthorhombic unit cell with $a = 0.742$ nm and $b = 0.601$ nm. The selective appearance of all four peaks indicated that the alkyl tails were tilted to a modest degree in the nearest neighbor direction. The appearance of the (2,1) peak paired with the absence of the (0,1) peak indicated a herringbone structure due to the two molecular locations in the unit cell being symmetrically inequivalent.

The inclusion of two dodecyl alkyl tails in the dendritic shell bought a reduction in the unit cell with an increase in long-range ordering. At all surface pressures, six sharp, intense peaks were observed in the diffraction patterns for **AA-2** (Figure 6a). The d-spacing for the two sharpest peaks were calculated at 0.412 and 0.371 nm and were indexed as the (1,1) and (2,0) peaks, respectively. The four additional higher Q_{xy} peaks were indexed as the (2,1), (0,2), (1,2), and (3,1) peaks at 0.299, 0.249, 0.236, and 0.222 nm, respectively. All peaks diminished in intensity at higher Q_z (larger azimuthal angle) GIXD patterns,

Monolayers of Photochromic Amphiphilic Monodendrons

J. Phys. Chem. B, Vol. 109, No. 43, 2005 **20397**
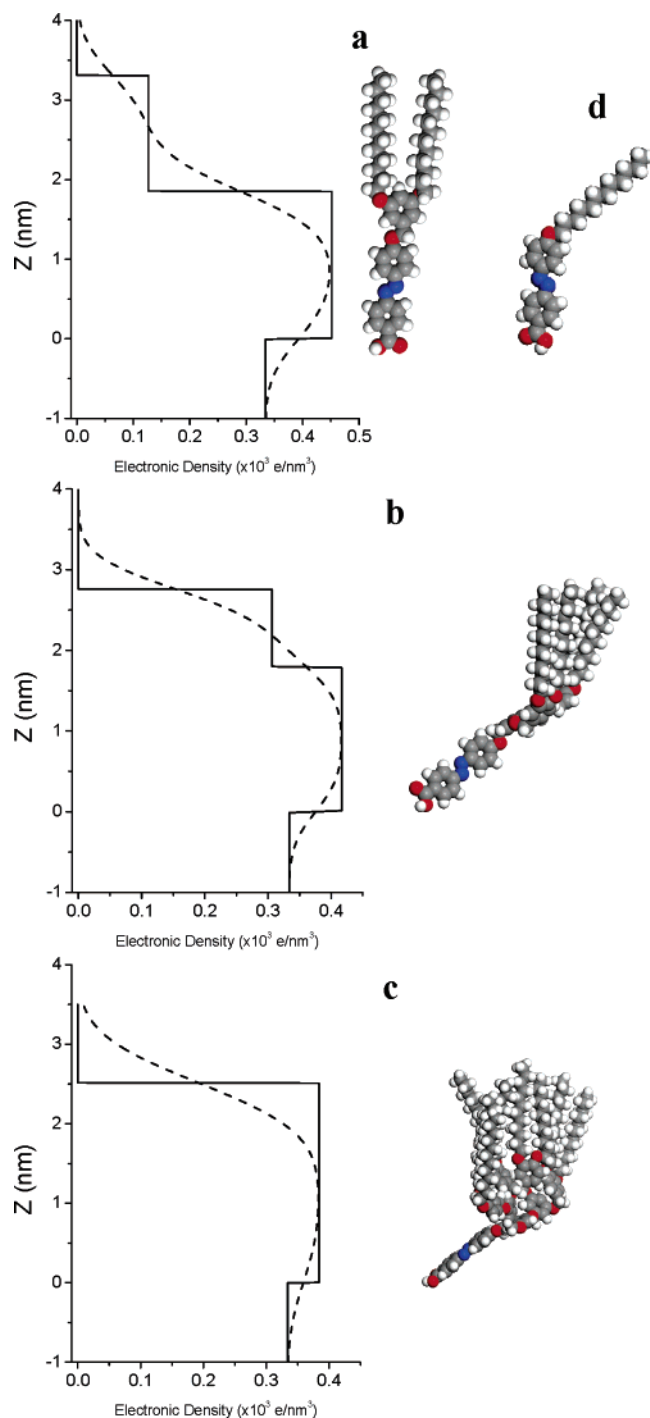

Figure 5. The box models calculated from X-ray reflectivity data shown in Figure 4 and molecular models with molecular dimensions matching density distribution for a) AA-2, b) AA-4 and c) AA-8 for the highest surface pressure (20mN/m). Model of AA-1 shown for comparison.[25]
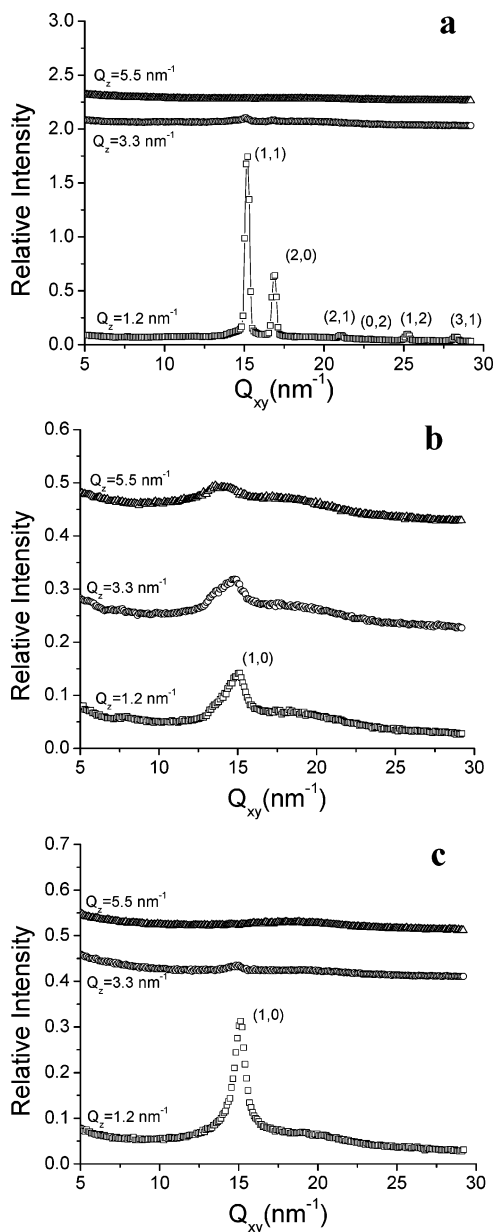

Figure 6. The GIXD patterns of the three highest generations observed for the Langmuir monolayers at 20 mN/m surface pressure. Data for higher azimutal angles is offset for clarity.

revealing that the alkyl tails are parallel to the surface normal. In contrast to the one tail molecule observed previously, the **AA-2** molecules formed a regular orthorhombic unit cell with no indication of a herringbone structure. The lattice parameters were calculated as $a = 0.742$ nm and $b = 0.495$ nm with the area per tail equal to 0.184 nm^2 (Table 1). The a lattice parameter calculated for both **AA-1** and **AA-2** was equal to 0.742 nm, while the b lattice parameter decreased approximately 0.1 nm from 0.601 nm for **AA-1** to 0.495 nm for **AA-2**.

A further increase in the number of alkyl tails disrupted the well-ordered orthorhombic lateral packing. A single broad peak

was observed at all surface pressures for **AA-4** and indexed as the (1,0) peak with a d-spacing of 0.420 nm (Figure 6b). The four tail molecule formed a quasi-hexagonal unit cell with the lattice parameter $a = 0.484$ nm and the area per tail 0.203 nm^2 (Table 1). Similarly, the eight tail molecule had a single broad peak at 0.418 nm, revealing that the alkyl tails formed a regular hexagonal lateral packing (Figure 6c). The lattice parameter decreased slightly to $a = 0.482$ nm, and the area per tail decreased to 0.201 nm^2 (Table 1). The reduction of the area per tail as the dendritic shell became bulkier (from four to eight tails) suggested that the alkyl tails of the larger molecule more readily rearranged at the air−water interface in a dense and vertical manner. As Q_z increased (larger azimutal angle), the observed peaks for **AA-4** and **AA-8** significantly decreased in intensity, strongly suggesting that the alkyl tails were parallel to the surface normal.

Comparisons of the correlation lengths for the most intense peaks of all four molecules indicated that the lower generation molecules had the highest long-range ordering. The correlation
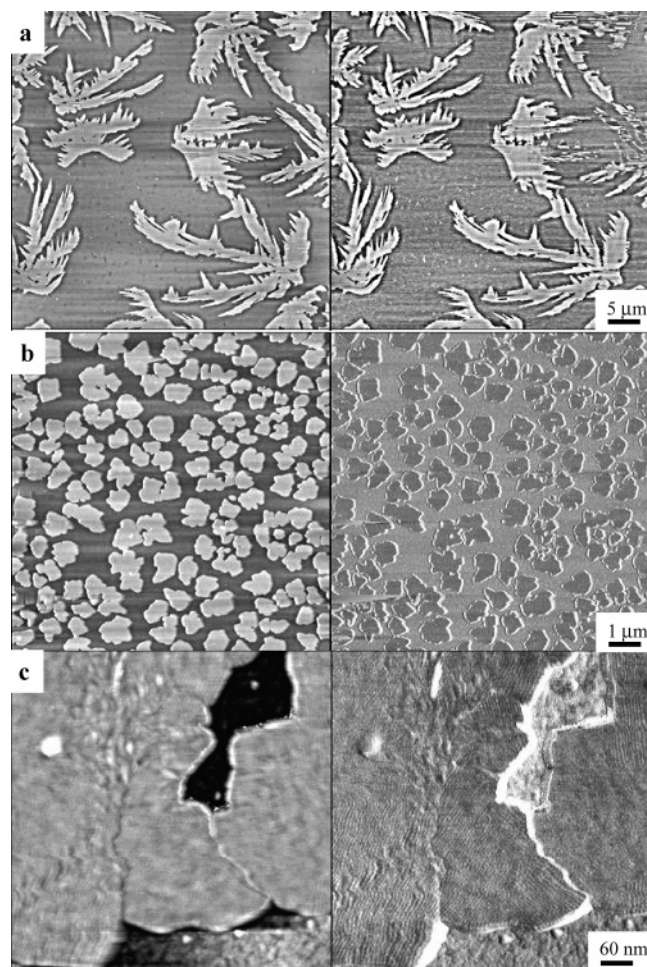
Figure 7. AA-2 formed irregular shaped domains with lateral dimensions of 1 micron and higher at all surface pressures as shown in AFM images. a) **AA-2** deposited at 3mN/m and b) at 20mN/m. c) High-resolution AFM image demonstrating lamellar structure observed within the domains shown in b). Scale: topography (L) and phase(R) for a) & b) z=10 nm and phase =40 degrees. For c) z=5 nm and phase=10 degrees.

TABLE 1: Comparison of Lattice Parameters of AA-N Calculated from GIXD

	AA-1	AA-2	AA-4	AA-8	AE-1
a (nm)	0.742	0.742	0.484	0.482	0.744
b (nm)	0.601	0.495			0.611
area per tail (nm^2)	0.223	0.184	0.203	0.201	0.227
tilt (deg)	26	0	0	0	42

lengths for the (1,1) and (2,0) peaks were 9.3 and 11.0 nm for **AA-1** and 10.0 and 10.4 nm for **AA-2**. In contract, the correlation lengths for the four and eight tail molecules decreased to 2.9 and 3.2 nm, respectively, determined from the (1,0) peak. The shift from the long-range ordering seen for the lower generation molecules to the limited short-range ordering for the two highest generations suggested that the crowded junction compromised the attached tails' ability to organize in the crystal lattice within the planar monolayer.

Further confirmation of the perpendicular arrangement of the alkyl tails of the higher generations was determined by analysis of rod scans of the most intense peaks of the three molecules (Figure 1S). The rod scans for the **AA-2** molecule in the (1,1) and (2,0) directions displayed a sharp peak prior to a gradual decrease in intensity. The modeling suggested a 2.9 nm rod parallel to the surface normal. The length of the rod was nearly twice that of a dodecyl alkyl tail, indicating that the molecule

TABLE 2: Comparison of Thickness of Solid and Liquid Supported Monolayers with Theoretical Lengths

	AFM	ellipsometry	XR	model
AA-1	1.9	3.1	2.8	2.9
AA-2	4.1	2.8	3.3	3.5
AA-4	NA	2.7	2.8	4.1
AA-8	NA	3.1	2.5	4.6
AE-1	1.9	3.3	2.6	3.1

is parallel to the surface normal up to the nitrogen double bond of the azobenzene spacer group. The rod scans for **AA-4** and **AA-8** in the (1,0) direction exhibited a similar trend (Figure 1S). The model resulted in a rod length less than the expected length for a dodecyl tail, indicating the lower portion of the tails being disordered. Apparently, the radial attachment of multiple tails to a single junction limited the ability of the alkyl tails to order beyond several molecules.

Surface Morphology at Solid Substrates. Evidence of the long-range ordering of the two tail molecules was observed for solid supported monolayers (Figure 7). At the lowest surface pressure, **AA-2** formed large leaf-like domains with overall lengths of several micrometers (Figure 7a). The thin arms of the leaf-like domains measured several hundred nanometers across. Upon increasing the surface pressure to 20 mN/m, the domains decreased in overall size and became more regularly shaped and densely packed (Figure 7b). The lateral dimension of the domains was approximately one μm. Higher resolution AFM of the solid supported monolayers deposited at higher surface pressures revealed that the domains were composed of a lamellae-like structure. Figure 7c illustrates the random orientation of the lamellae structure (more clearly observed in the phase image) with the shift in the directional organization inside of the domain. The d spacing was calculated to be 5.7 nm, indicating interdigitated bilayer packing similar to that observed for crown-containing monodendrons.[13a]

The limited short range ordering of **AA-4** and **AA-8** was evident for monolayers deposited at all surface pressures. The four and eight tail molecules formed uniform monolayers with very limited areas of short lamellae-like structures (Figure 2S). The lower than expected effective thickness of the monolayers suggested that the focal group of the higher generation molecules was significantly tilted from the surface normal (Table 2). The cross-sectional area of the dendritic shell for **AA-4** and **AA-8** was 3−6 times larger than the cross-sectional area of the acid headgroup, thus creating a large mismatch. This allowed the focal group fragment to adopt large tilt angles, thereby greatly reducing the monolayer thickness.

Comparison of monolayer thickness at the air−water and air−solid interface to the estimated length from molecular model concluded that the inclusion of multiple alkyl tails in the dendritic shell, particularly four and eight tails, forced the molecules to adopt a tilted orientation (Table 2). Previous studies demonstrated that **AA-1** oriented perpendicular to the surface as the **AE-1** molecules formed a kinked structure.[25] The good agreement observed between the estimated length of the **AA-2** from molecular models and the liquid and solid supported monolayers confirm a similar parallel orientation to the surface normal for the two tail molecule. The lower effective thickness of the solid supported monolayer of **AA-2** was attributed to the domain structure observed by AFM. The thickness of liquid and solid supported monolayers was significantly lower than the estimate length of the molecular models for **AA-4** and **AA-8**. Comparison of the length of the tail box from X-ray reflectivity and the length estimated from the rod scans suggested that the lower third of the alkyl tails was disordered
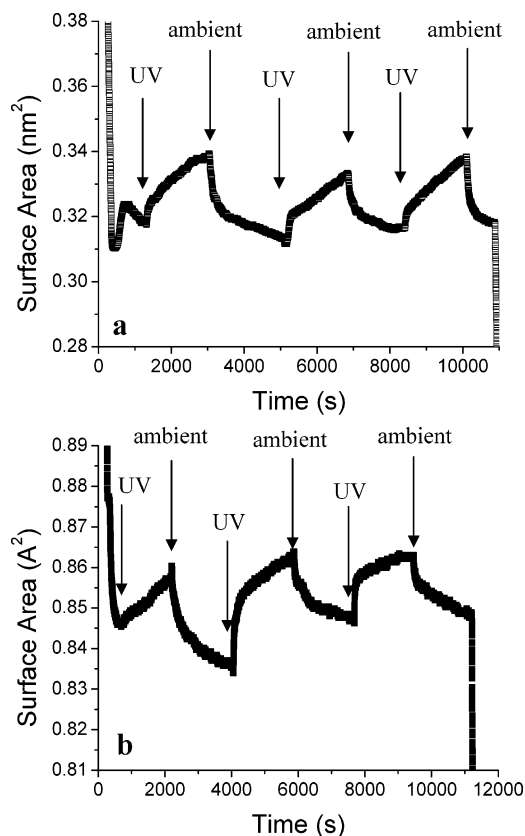
Monolayers of Photochromic Amphiphilic Monodendrons

J. Phys. Chem. B, Vol. 109, No. 43, 2005 **20399**

Figure 8. Variation of molecular area versus time for a) **AA-2** and b) **AA-4** as the Langmuir monolayer was exposed to repeated cycles of 365 nm and ambient light. Arrows show source of illumination.

Figure 9. X-ray reflectivity for a) AA-2 and b) AA-4 monolayers at all surface pressures under 365 nm illumination. Data and model represented by symbols and lines, respectively.

due to the close association to the phenyl rings in the dendritic shell. The larger cross-sectional mismatch of the higher generations (**AA-4** and **AA-8**) resulted in a kinked structure at interfaces with azobenzene groups lying virtually parallel to the solid surface, similar to the previously studied **AD12-N** molecules.[15]

Photoisomerization within Langmuir Monolayers. The question of the preservation of the reversible photoisomerization in the monolayer state is important for the fabrication of surface monolayers at solid surfaces. The photoisomerization of the lower generation monodendrons was studied at the air–water interface to determine the mobility of the molecules in loosely packed two-dimensional monolayer films (Figure 8). The selected Langmuir monolayers were compressed to 10 mN/m and exposed to repeated cycles of 365 nm light and ambient light as the surface pressure was held constant. Kinetic studies of one and eight tail molecules at the air–water interface were not preformed due to stability concerns. The four tail molecule exhibited a very modest 3.5% rise in molecular area upon UV illumination. In contrast, the **AA-2** molecule had an 8.8% molecular area increase for the monolayer UV illuminated for several minutes with gradual relaxation to the initial value (Figure 8). The smaller difference in cross-sectional area for the **AA-4** monolayer indicated the inability of the molecules to fully achieve complete photoisomerization transitions due to the densely packed alkyl tails. The cross-sectional mismatch of the four alkyl tails attached to the azobenzene spacer group and the smaller carboxylic focal group allowed for significant rearrangement of the focal group fragment without considerably affecting the ordering of the alkyl tails. The large difference in the molecular area for the **AA-2** molecule observed for the trans and cis isomers denotes that the two tail molecules possess the preferential cross-section mismatch to preserve the photoisomer-
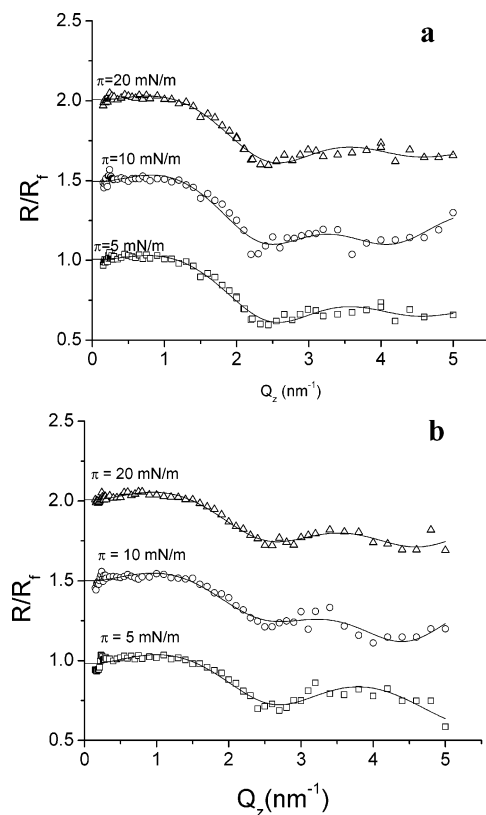
ization of the molecules within the densely packed monolayer at the air–water interface.

The two and four tail molecules were further analyzed by X-ray reflectivity under UV illumination to elucidate the ordering of the molecules in the cis isomer. Although the reference molecule **AE-1** demonstrated a similar trend in molecular area during the UV kinetics studies as **AA-4**, the molecules proved unstable under UV illumination at the air–water interface on the time scale of the X-ray reflectivity experiments. Surprisingly, the X-ray reflectivity data for monolayers of **AA-2** and **AA-4** exposed to UV illumination indicated more uniform films with a slight decrease in the overall film thickness as compared to the trans-state of azobenzene groups (Table 1S). The data for both molecules have one defined minimum at lower Q_z with additional less defined minima at higher Q_z (Figure 9). The defined minima shifted slightly to a lower Q_z value at moderate pressure in comparison to a higher Q_z position for lower and higher surface pressure for the two and four tail molecule.

A two-box model of electron density distribution was used for all pressures for both molecules with a similar assignment of the molecular fragments as used for the monolayers analyzed under ambient conditions (the trans-state of azobenzene groups). The headgroup box with elevated electron density for the two tail molecule in the cis-state was similar in length to that under the ambient light (Table 1S and Figure 10). However, the electronic density decreased significantly, from 12.5% for the lowest surface pressure to 22% for the highest surface pressure, due to a larger molecular area observed for the UV illuminated monolayer. In contrast, the length of the tail box was 22% lower for the UV illuminated monolayers, and the electronic density was slightly lower than expected for densely packed alkyl tails (Figure 10a and Table 1S), suggesting that the alkyl tails tilt
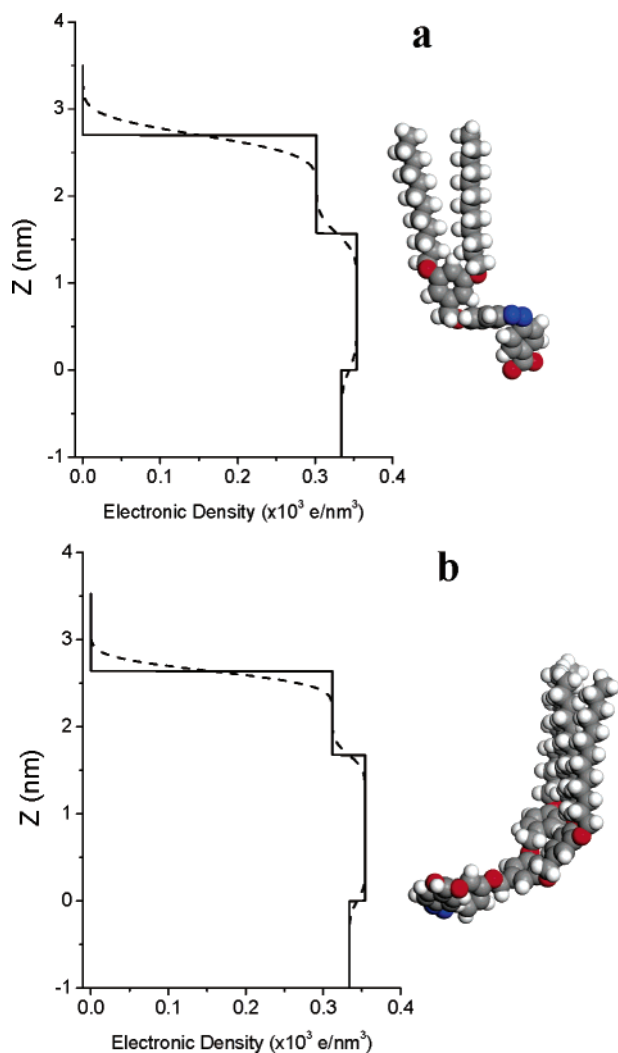
Figure 10. The electron density distribution models calculated from data shown in Figure 11 for a) AA-2 and b) AA-4 monolayers under 365 nm illumination at the highest surface pressure (left) and molecular models (right).

during the molecular reorganization. Unlike monolayers observed under ambient conditions, the alkyl tail box of the UV illuminated monolayer remained relatively consistent, indicating a more stable monolayer.

The attachment of four tails to the azobenzene group changed the surface behavior significantly. Comparison of the box models of **AA-4** for trans and cis states of the azobenzene groups showed similar trends in the molecular ordering (Figures 5c and 9b and Table 1S). Overall, the electronic density of the focal group box was reduced 20% as the length increased slightly (<5%) for the cis isomer monolayer, correlating with the larger molecular area observed for the stimulated monolayer. Compressing the monolayer to moderate surface pressure exhibited an approximate 38% elongation of the focal group box as the tail box length was reduced 6% for ambient conditions to 33% for the UV illuminated monolayer. Unlike the ambient condition monolayers, the alkyl tails attached to the cis isomer adopted a tilted behavior to recover the enlarged molecular area.

Photoisomerization within Chemically Grafted Layers. Finally, the photoisomerization of the two tail molecule **AA-2** with the largest variation of cross-sectional area upon UV illumination was analyzed after chemical grafting of these molecules to the solid substrate. Direct comparison was done
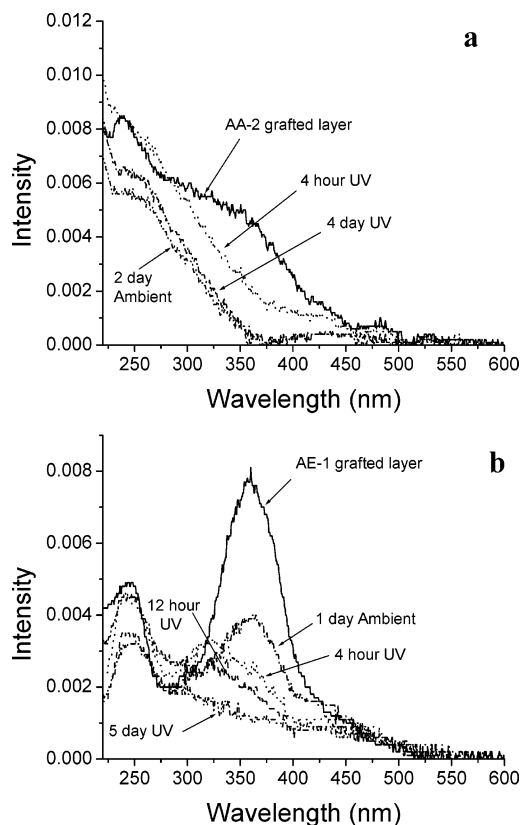

Figure 11. Kinetic studies of the photoisomerization of grafted films of a) **AA-2** and b) **AE−1**.

with an epoxy-terminated single-chain molecule designed for direct chemical grafting, **AE-1**.[25] The substrate for **AA-2** was first functionalized with a poly(ethylene imine) (PEI) monolayer using a previous reported experimental procedure to assist the grafting of the carboxyl terminated molecules.[26] The epoxy terminated reference sample formed a uniform layer with a few small hole defects (<100 nm diameter) and particle contaminants within a 1 μm square region. The 5.7 nm depth of the layer defects suggested a possible bilayer structure, while the 2.8 nm height of the particle contaminants indicates that additional molecules remained on the surface after rinsing. The **AA-2** molecule formed a similar uniform layer with significantly more, larger particle contaminants. The 3.9 nm thickness determined by AFM cross-sections indicates a grafted monolayer. As in previous studies of photoisomerization of solid support monolayers, the grafted **AA-2** films exhibited a fine texture before photoisomerization that was disrupted after photoisomerization.[27]

A broad, asymmetric peak was observed at 365 nm for the grafted **AA-2** layer, indicating the characteristic $\pi-\pi^*$ absorption band in addition to a smaller peak observed at 250 nm previously attributed to the additional phenyl ring in the dendritic shell (Figure 11). The asymmetry of the peaks was attributed to constructive interference of the background peak of the PEI film. After 4 h illumination of 365 nm UV light in a dark environment, the absorption bands at 250 and 365 nm decreased with complete dissipation of the 365 nm peak after 4 days of illumination. The grafted film of the **AA-2** molecules showed weak indications of cis to trans isomerization. After 2 days relaxation in a dark environment, the grafted films were exposed to ambient light for 24 h to determine if relaxation would occur under dark conditions or if only stimulated by favorable light. Comparison of the UV−vis spectra for the **AA-2** and **AE-1**

Monolayers of Photochromic Amphiphilic Monodendrons

J. Phys. Chem. B, Vol. 109, No. 43, 2005 **20401**

molecules revealed that the epoxy terminated reference sample had improved photoisomerization capabilities for grafted thin films.

The grafted films of **AE-1** exhibited a broad absorption band at 365 nm, corresponding to the $\pi-\pi*$ band and an additional band at 250 nm. After 4 h illumination, the peaks at 365 and 250 nm were significantly reduced, and a less intense, broader peak appeared at 455 nm, signifying a nearly 80% photoisomerization of the grafted layer (Figure 11). After 5 days of UV illumination, the 365 nm absorption band was completely dissipated, and low intensity peaks were observed at 250 and 455 nm, indicating a complete transformation from trans to cis isomers. After 2 days of relaxation, the grafted film of **AE-1** underwent a partial transformation from cis to trans isomers (Figure 11). The grafted films of the epoxy terminated reference molecule achieved approximately 50% transformation after 1 day of relaxation in ambient light.

Conclusions

Previously, we demonstrated that a large cross-sectional mismatch between a bulky polar head and a varying number of alkyl tails in the dendritic shell force the molecules to adopt kinked structures to form densely packed ordered structures.[15b] The single alkyl tail molecule formed a supercell orthorhombic packing structure due to the significant tilt of the alkyl tails caused by the azobenzene spacer group and the bulky crown ether head alternately stacking within the monolayer. As observed here, the previous molecules formed less ordered structures as the number of alkyl tails increased in the dendritic shell. We demonstrated that the four tail molecule with a crown ether polar group reorganized in solid supported films by the disruption of oriented stripes after photoisomerization. A similar disruption in ordering was observed for grafted films of the two tail molecule with the carboxylic acid group here.[27] The homogeneous fine texture of the **AA-2** grafted films became a disorganized and heterogeneous film after photoisomerization. Similar disruption in texture for crystalline phases during photoisomerization has been observed for carbosilane dendrimers in spin cast and annealed thin films.[28]

Functionalizing dendrimers with azobenzene terminal groups to improve the fragment spacing required to preserve the photoisomerization within monolayers was shown to have similar behavior as low molar weight surfactants but had a higher probability of interaction of the azobenzene groups of neighboring molecules.[29] Similar to the monodendrons shown here, the generation number of carbosilane dendrimers with azobenzene groups at the periphery had little effect on the photoisomerization of the mesogenic groups is solution.[30] The photochromic behavior of the terminal groups was affected by the crystalline structure induced by the film preparation. The amorphous structure of the spin cast films caused overlapping of the azobenzene groups of neighboring molecules forming H aggregates, whereas the photoisomerization behavior in the crystalline films was similar to low molar mass compounds. Attraction between azobenzene terminal groups to interdigitate forced highly polar cores of dendrimers to flatten and form multilaminar vesicles in solution, similar in behavior to low molar weight surfactants.[31]

The replacement of the traditional carboxylic polar head with the epoxy group increased the cross-sectional area of the molecule in addition to broadening the orthorhombic unit cell of the alkyl tails. Similar to the lowest generations of the **AA-N** molecules, the epoxy functionalized molecule formed a herringbone structure with reasonable long-range ordering.

Unlike the **AA-1** and **AA-2** molecules that ordered parallel to the surface normal, the **AE-1** reference molecule formed a kinked structure similar to the previously studied molecules with a larger polar group.[15] Although **AE-1** displayed limited molecular area differences during photoisomerization in Langmuir monolayers, the photoisomerization of the grafted layers of the epoxy terminated reference molecule was more successful than for the **AA-2** molecule.

In addition to the variance of molecular area during photoisomerization, we directly observed the trans−cis photoisomerization in a Langmuir film in situ using X-ray reflectivity. The 8% increase in molecular area observed for cis **AA-2** reduced the monolayer thickness as the molecule kinked, thereby disrupting the perpendicular orientation of the entire molecule. Unlike the two tail molecule, the **AA-4** molecules displayed less molecular rearrangement due to the cross-sectional area controlled by the four alkyl tails. The area available for the focal group is twice the required space; therefore, the fragment reorientation had little effect on the monolayer structure. The packing density of the azobenzene fragment in Langmuir−Blodgett monolayers has been shown to affect the degree of photoisomerization of the surface films.[8] Although the larger dendritic shell preserved the cross-sectional area for the photoisomerization, it limited the observed effect due to the cross-sectional mismatch greatly favoring the alkyl tails.

The influence of the dendritic shell containing multiple dodecyl tails has been discerned to assert a great effect on the higher generations versus the influence of a bulky azobenzene spacer group that affected the lower generations. The influence of the azobenzene is directional determined by the decrease in the *b* lattice parameter upon the increase in the alkyl shell from one to two tails. The four and eight tail molecules formed uniform monolayers with limited short-range ordering seen in liquid and solid supported films. The highest generations adopted a kinked structure with the alkyl tails parallel to the surface normal, while the focal group was tilted a large degree toward the surface as seen as an overall decrease in effective thickness of deposited films.

All molecules were capable of repeated photoisomerization in dilute solutions under preferential light conditions. At the air−water interface, the two tail molecule possessed the ideal cross-sectional mismatch that facilitated the trans to cis isomerization and retained the mobility for the cis to trans isomerization for specific stimuli. The **AA-4** and **AE-1** molecules exhibited a limited photoisomerization response at the air−water interface. Conversely, kinetics studies of grafted thin films revealed that although both the **AA-2** and the **AE-1** molecules showed complete trans to cis isomerization, only the epoxy terminated reference molecule was observed to partially transform from cis to trans. The importance of the range of mobility of the molecules was shown in the increased time scale of the kinetics experiments from dilute solutions to liquid supported monolayers to thin films grafted to solid substrates.

20402 *J. Phys. Chem. B, Vol. 109, No. 43, 2005*

Genson et al.

Supporting Information Available: Full description of experimental details for home-built liquid−surface reflectometer, table of parameters of the box models calculated X-ray reflectivity data for **AA-N**, data and models for rod scans of **AA-N**, and AFM images of deposited monolayers of **AA-4** and **AA-8**. This material is available free of charge via the Internet at http://pubs.acs.org.

References and Notes

(1) (a) Julthongpiput, D.; Lin, Y.-H.; Teng, J.; Zubarev, E. R.; Tsukruk, V. V. *J. Am. Chem. Soc.* **2003**, *125*, 15912. (b) Luzinov, I.; Minko, S.; Tsukruk, V. V. *Prog. Polymer Sci.* **2004**, *29*, 635. (c) Tsukruk, V. V. *Prog. Polymer Sci.* **1997**, *22*, 247.

(2) (a) Ikeda, T. *J. Mater. Chem.* **2003**, *13*, 2037. (b) Nishihara, H. *Bull. Chem. Soc. Jpn.* **2004**, *77*, 407. (c) Shibaev, V.; Borbovsky, A.; Boiko, N. *Prog. Polymer Sci.* **2003**, *28*, 729. (d) Seki, T. in *Handbook of Photochemistry and Photobiology*; Nalwa, H. S., Ed.; American Scientific Publishers: Stevenson Ranch, CA, 2003; p 435.

(3) (a) Rochon, P.; Batalla, E.; Natanson, A. *Appl. Phys. Lett.* **1995**, *66*, 136; (b) Kim, D. Y.; Tripathy, S. K.; Li, L.; Kumar, J. *Appl. Phys. Lett.* **1995**, *66*, 1166.

(4) Kawata, S.; Kawata Y. *J. Opt. Soc. Am. B* **2001**, *18*, 1777.

(5) (a) Meng, X.; Natansohn, A.; Barrett, C.; Rochon, P. *Macromolecules* **1996**, *29*, 946; (b) Ho, M.; Natansohn, A.; Barrett, C.; Rochon, P. *Can. J. Chem.* **1995**, *73*, 1773; (c) Natansohn, A.; Rochon, P.; Ho, M.; Barrett, C. *Macromolecules* **1995**, *28*, 4179.

(6) Ichimura, K. *Chem. Rev.* **2000**, *100*, 1847.

(7) Yamaoka, T.; Makita, Y.; Sasatani, H.; Kim, S.-I.; Kimura, Y. *J. Contr. Release* **2000**, *66*, 187.

(8) (a) Seki, T.; Kojima, J.; Ichimura, K. *Macromolecules* **2000** *33*, 2709; (b) Seki, T.; Sekizawa, H.; Fukuda, R.; Tamaki, T.; Yokoi, M.; Ichimura, K. *Polymer J.* **1996** *28*, 613; (c) Seki, T.; Sekizawa, H.; Fukuda, R.; Morino, S.; Ichimura, K. *J. Phys. Chem.* **1998**, *102*, 5313; (d) Seki, T.; Fukuda, R.; Tamaki, T.; Ichimura, K. *Thin Solid Films* **1994**, *243*, 675; (e) Seki, T.; Sakuragi, M.; Kawanishi, Y.; Suzuki, Y.; Tamaki, T. *Langmuir* **1993**, *9*, 211.

(9) Siewierski, L. M.; Brittain, W. J.; Petrash, S.; Foster, M. D. *Langmuir* **1996**, *12*, 5838.

(10) (a) Newkome, G. R.; Moorefield, C. N.; Vogtle, F. (Ed.), *Dendritic Molecules*, VCH: Weinheim, **1996**; (b) Frechet, J. M. *Science* **1994**, *263*, 1711; (c) Tully, D. C.; Frechet, J. M. *J. Chem. Communications,* **2001**, 1229; (d) Kampf, J. P.; Frank, C. W. *Langmuir*, **1999**, *15*, 227.

(11) (a) Seiler, M. *Chem. Eng. Technol.* **2002**, *25*, 3; (b) Vogtle, F.; Gestermann, S.; Hesse, R.; Schwierz, H.; Windisch, B. *Prog. Polym. Sci.* **2000**, *25*, 987; (c) Grayson, S. M.; Frechet, J. M. *Chem. Rev.* **2001**, *101*, 3819; (d) Pyun, J.; Zhou, X.-Z.; Drockenmuller, E.; Hawker, C. J. *J. Mater. Chem.* **2003**, *13*, 2653; (e) Frechet, J. M. J. *J. Polym. Sci. A: Polym. Chem.* **2003**, *41*, 3713.

(12) (a) Percec, V.; Cho, W. D.; Mosier, P. E.; Ungar, G.; Yeardley, D. J. P. *J. Am. Chem. Soc.* **1998**, *120*, 11061; (b) Balagurusamy, V. S. K.; Ungar, G.; Percec, V.; Johansson, G. *J. Am. Chem. Soc.* **1997**, *119*, 1539; (c) V. Percec, C. H. Ahn, W. D. Cho, A. M. Jamieson, J. Kim, T. Leman, M. Schmidt, M. Gerle, M. Moller, S. A. Prokhorova, S. S. Sheiko, S. Z. D. Cheng, A. Zhang, G. Ungar, D. J. P. Yeardely, *J. Am. Chem. Soc.* **1998**, *120*, 8619. (d) Percec, V.; Cho, W.-D.; Ungar, G. *J. Am. Chem. Soc.* **2000**, *122*, 10273; (e) Percec, V.; Cho, W.-D.; Ungar, G.; Yeardley, D. J. P. *J. Am. Chem. Soc.*, **2001**, *123*, 1302; (f) Guillon, D.; Deschenaux, R. *Curr. Opin. Solid State Mater. Sci.* **2002**, *6*, 515. (g) Tully, D. C.; Frechet, J. M. J. *Chem. Commun.* **2001**, 1229; (h) Brunsveld, L.; Folmer, B. J. B.; Meijer, E. W.; Sijbesma, R. P. *Chem. Rev.* **2001**, *101*, 4071.

(13) (a) Peleshanko, S.; Sidorenko, A.; Larson, K.; Villavicencio, O.; Ornatska, M.; McGrath, D. V.; Tsukruk, V. V. *Thin Solid Films* **2002**, *406*, 233; (b) Sidorenko, A.; Houphouet-Boigny, C.; Villavicencio, O.; McGrath, D. V.; Tsukruk, V. V. *Thin Solid Films* **2002**, *410*, 147.

(14) (a) Mindyuk, O. Y.; Heiney, P. A. *Adv. Mater.* **1999**, *11*, 341. (b) Mindyuk, O. Y.; Stetzer, M. R.; Heiney, P. A.; Nelson, J. C.; Moore, J. S. *Adv. Mater.* **1998**, *10*, 1363. (c) Heiney, P. A.; Stetzer, M. R.; Mindyuk, O. Y.; DiMasi, E.; McGhie, A. R.; Liu, H.; Smith, A. B. *J. Phys. Chem. B* **1999**, *103*, 6206. (d) Gidalevitz, D.; Mindyuk, O. K.; Stetzer, M. R.; Heiney, P. A.; Kurnaz, M. L.; Schwartz, D. K.; Ocko, B. M.; McCauley, J. P.; Smith, A. B. *J. Phys. Chem. B* **1998**, *102*, 6688.

(15) (a) Larson, K.; Vaknin, D.; Villavicencrio, O.; McGrath, D. V.; Tsukruk, V. V. *J. Phys. Chem.* **2002**, *106*, 7246; (b) Genson, K. L.; Vankin, D.; Villavicencio, O.; McGrath, D. V.; Tsukruk, V. V. *J. Phys. Chem.* **2002**, *106*, 11277.

(16) Vaknin, D. in: *Methods of Materials Research*, Eds. Kaufmann, E. N.; Abbaschian, R.; Baines, P. A.; Bocarsly, A. B.; Chien, C. L.; Doyle, B. L.; Fultz, B.; Leibowitz, L.; Mason, T.; Sanches, J. M. **2001**, John Wiley & Sons: New York, p 10d.2.1

(17) Weissbuch, I.; Leveiller, F.; Jacquemain, D.; Kjaer, K.; Als-Nielsen, J.; Leiserowitz. L. *J. Phys. Chem.* **1993**, *97*, 12858.

(18) Vaknin, D.; Kelley, M. S. *Biophys. J.* **2000**, *79*, 2616.

(19) Bliznyuk, V. N.; Everson, M. P.; Tsukruk, V. V. *J. Tribology* **1998**, *120*, 489.

(20) Tsukruk, V. V. *Adv. Mater.* **2001**, *13*, 95.

(21) Ulman, A. An Introduction to Ultrathin Organic Films, Academic Press: San Diego, CA **1991**.

(22) (a) Tsukruk, V. V. *Rubber Chem. Techn.* **1997**, *70(3)*, 430; (b) Tsukruk, V. V.; Reneker, D. H. *Polymer* **1995**, *36*, 1791; (c) Ratner, B.; Tsukruk, V. V. (Eds.) *Scanning Probe Microscopy of Polymers*, ACS Symposium Series, v. 694, **1998**.

(23) Villavicencio, O. F.; McGrath, D. V., in preparation.

(24) (a) Kumar, G. S.; Neckers, D. C. *Chem. Rev.* **1989**, *89*, 1915; (b) Irie, M.; Ikeda, T. in *Functional Monomers and Polymers (2nd Edition)*, Takemoto, K.; Ottenbite, R.; Kamachi, M. (Eds.) Dekker: New York, 1997.

(25) Genson, K. L.; Holzmueller, J.; Villavicencio, O.; McGrath, D.; Tsukruk, V. V. *Thin Solid Films* **2005**, in print.

(26) (a) Jiang, C.; Markutsya, S.; Tsukruk, V. V. *Adv. Mater.* **2004**, *16*, 157; (b) Cho, J.; Char, K.; Hong, J.-D.; Lee, K.-B. *Adv. Mater.* **2001**, *13*, 1076; (c) Chiarelli, P. A.; Jonal, M. S.; Carron, J. L.; Roberts, J. B.; Robinson, J. M.; Wang, H.-L. *Langmuir* **2002**, *18*, 168.

(27) Tsukruk, V. V.; Luzinov, I.; Larson, K.; Li, S.; McGrath, D. V. *J. Mater. Sci. Lett.* **2001**, *20*, 873.

(28) Bobrovsky, A. Yu.; Pakhomov, A. A.; Shu, X.-M.; Boiko, N. I.; Shibaev, V. P.; Stumpe, J. *J. Phys. Chem. B* **2002**, *106*, 540.

(29) Weener, J.-W.; Meijer, E. W. *Adv. Mater.* **2000**, *12*, 741.

(30) Bobrovosky, A.; Ponomarenko, S.; Boiko, N.; Shibaev, V.; Rebrov, E.; Muzafarov, A.; Stumpe, J. *Macromol. Chem. Phys.* **2002**, *203*, 1539.

(31) Tsuda, K.; Dol, G. C.; Gensch, T.; Hofkens, J.; Latterini, L.; Weener, J. W.; Meijer, E. W.; De Schryver, F. C. *J. Am. Chem. Soc.* **2000**, *122*, 3445.